Virology 407 (2010) 120–128

Contents lists available at ScienceDirect

Virology

journal homepage: www.elsevier.com/locate/yviro

Discovering microRNAs from *Bombyx mori* nucleopolyhedrosis virus

J. Singh, C.P. Singh, A. Bhavani, J. Nagaraju *

Centre of Excellence for Genetics and Genomics of Silkmoths, Laboratory of Molecular Genetics, Centre for DNA Fingerprinting and Diagnostics, Tuljaguda Complex, Mozamjahi Road, Nampally, Hyderabad 500001, India

ARTICLE INFO

Article history:
Received 28 May 2010
Returned to author for revision 17 June 2010
Accepted 20 July 2010
Available online 30 August 2010

Keywords:
miRNAs
BmNPV
Baculovirus
Bombyx mori

ABSTRACT

MicroRNAs (miRNAs) have emerged as key players in host–pathogen interaction. Recently, many virus-encoded miRNAs have been identified from different mammalian species. However, the large family of invertebrate viruses of Baculoviridae, which infects diverse species of beneficial insects and agriculture pests, has hardly been investigated for elucidating the role of miRNAs in host–pathogen interaction.

In the study reported here, we have identified four *Bombyx mori* nucleopolyhedrosis virus (BmNPV)-encoded miRNAs using a combination of *in silico* and experimental methods. Unlike other reported viral miRNAs, the BmNPV-encoded miRNAs identified in the present study were found to be evolutionarily conserved among many closely related baculoviruses.

Besides, we have computationally predicted 8 viral and 64 cellular targets of these virus-encoded miRNAs and the putative functions of these targets suggest a key role of viral miRNAs in insect-pathogen interactions by modulating several viral replication genes as well as those involved in host immune defense machinery.

Introduction

MicroRNAs are endogenous, non-coding RNAs of ~22 nucleotides that regulate gene expression in a sequence-specific manner. These regulatory RNAs are processed from ~80 nucleotide long, stem-loop structured precursor miRNAs (pre-miRNAs), which are derived from the cleavage of primary miRNA transcripts (pri-miRNAs) (Lee et al., 2002) in the nucleus by an RNase III enzyme, Drosha (Lee et al., 2003). Exportin 5, an export factor (Yi et al., 2003) helps in the transport of these pre-miRNAs to the cytoplasm, where they are recognized and processed by another RNase III, Dicer (Grishok et al., 2001; Hutvagner et al., 2001; Ketting et al., 2001) into miRNA::miRNA* duplexes, which then unwind and one of the strands gets incorporated into RNA-induced silencing complex (RISC) (Schwarz et al., 2004). This assembly of RISC and miRNA binds to the target mRNA and depending upon the extent of complementarity results in either degradation or translational repression of the target mRNA (Lau et al., 2001; Bartel, 2004). Since the first discovery of miRNA in *Caenorhabditis elegans* (Lee et al., 1993; Reinhart et al., 2000), thousands of miRNAs have been identified from a broad range of multicellular organisms. Recent reports suggest that viruses too encode miRNAs for regulating both viral and cellular genes involved in host–virus interaction (Gupta et al., 2006; Murphy et al., 2008; Sullivan and Ganem, 2005a,b; Triboulet et al., 2007).

The viral miRNAs were first discovered in the herpesvirus, Epstein–Barr virus (EBV) (Pfeffer et al., 2004) and till date more than 200 virus-encoded miRNAs have been reported as per the miRNA registry, miRBase (Release 15) (Griffiths-Jones, 2004). Except for the recent report of just one insect virus-encoded miRNA of *Heliothis virescens* ascovirus (HvAV) (Hussain et al., 2008), all virus-encoded miRNAs identified till date are from mammalian viruses. In the study reported here, we have identified and characterized four miRNAs from the domesticated silkmoth, *Bombyx mori*-specific baculovirus, *B. mori* nucleopolyhedrosis virus (BmNPV). Baculoviruses belong to a large and diverse group of double-stranded DNA viruses, which include many devastating pathogens infectious to several economically important arthropods, particularly insects of the order Lepidoptera (Rohrmann, 2008). *B. mori* is a Lepidopteran model system for genetics and molecular studies. BmNPV is a natural pathogen of *B. mori*, which inflicts a very high mortality on *B. mori* resulting in heavy silk cocoon loss, thus causing a major economic damage to the silk industry. The availability of complete genome sequence of *B. mori* (480 Mb) and BmNPV (128 Kb), and the functional analysis of genes involved in BmNPV infection and proliferation provides us the requisite handle to investigate the molecular mechanisms involved in host–pathogen interaction.

Generally, approaches based on phylogenetic conservation of sequences across multiple species are known to provide reliable indicators for the prediction of functional miRNAs (Stark et al., 2007a, b), but this may not be the case with viruses, because, unlike host miRNAs, virus-encoded miRNAs show no or very low sequence similarity with each other (Pfeffer et al., 2005, 2004). Hence, we set out to identify the virus-encoded miRNAs by using well-established

* Corresponding author. Fax: +91 40 24749343.
E-mail addresses: jyotis@cdfd.org.in (J. Singh), cpsingh@cdfd.org.in (C.P. Singh), bhavani@cdfd.org.in (A. Bhavani), jnagaraju@cdfd.org.in (J. Nagaraju).

0042-6822/$ – see front matter © 2010 Elsevier Inc. All rights reserved.
doi:10.1016/j.virol.2010.07.033

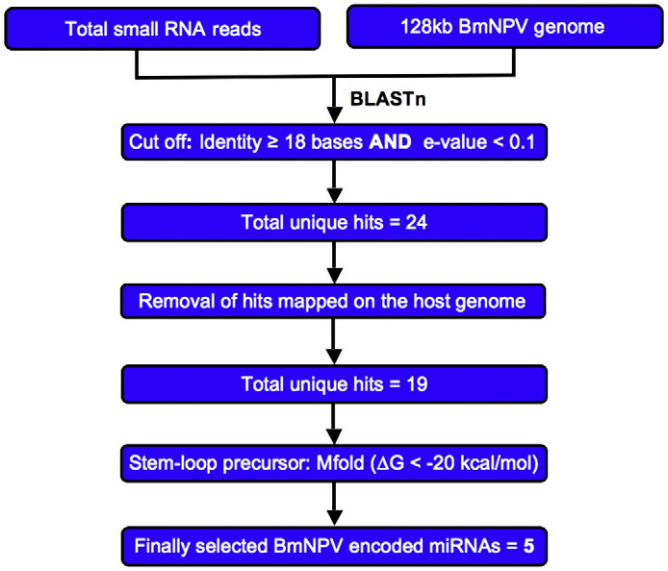

Fig. 1. Bioinformatics data analysis pipeline for the prediction of BmNPV-encoded miRNAs.

experimental methods, which include isolation of small RNAs from infected tissues followed by cDNA cloning, pyro-sequencing and *in silico* sequence analyses (Bennasser et al., 2004; Pfeffer et al., 2005, 2004). The putative miRNAs were then experimentally validated by techniques like Northern blot, stem-loop RT-PCR (Chen et al., 2005; Ro et al., 2006; Varkonyi-Gasic et al., 2007; Yu et al., 2008) and poly (A)-tailed RT-PCR (Fu et al., 2006). Interestingly, all the four validated miRNAs were found to be evolutionarily conserved in the closely related baculoviruses, which infect different insects that have diverged several million years ago.

We have also attempted to computationally predict the putative targets of these miRNAs by employing miRanda program (Enright et al., 2003) along with stringent screening using different filters based on several important statistical parameters. Efforts are underway in our lab to experimentally validate these targets.

We believe that these BmNPV-encoded miRNAs and their putative targets will serve as useful resources for initiating studies to understand the molecular mechanisms involved in host–pathogen interaction, which would enable us to develop a durable, effective and non-toxic antiviral therapy using miRNA against BmNPV infection in *B. mori*.

Results and Discussion

Prediction of miRNAs from BmNPV

We chose to examine the expression profile of viral miRNAs in midgut and fat body tissues for the following reasons: 1) BmNPV initiates infection in the insect midgut columnar epithelial cells and hence, one can expect high level expression of viral miRNAs to manoeuvre the host defense components like phenoloxidase cascade (Cerenius and Soderhall, 2004), 2) Fat body tissues are spread throughout the larval body and considered to be the major immune organ in insects. During viral infection, very active proliferation of virus occurs in the fat body tissues (Bulet et al., 2004; Hultmark et al., 1980; Yamakawa and Tanaka, 1999).

In the present study, we generated about 70,000 small RNA sequence reads from each of these two infected tissues using GS FLX sequencing. Total population of small RNAs recovered from each of the infected tissues is given in Table S2 of supplementary file1. These sequences were further sorted for potential viral miRNAs by employing many important filters based on published work (Cai et al., 2005; Pfeffer et al., 2005, 2004). An overview of bioinformatics data analysis pipeline is shown in Fig. 1. A total of 58900 small RNA sequences from infected fat body and 64463 from infected midgut were mapped on to the BmNPV genome sequence using BLASTn program (Altschul et al., 1990). The search resulted in 24 distinct small RNA hits (after removal of duplicate hits), 17 from the fat body and 7 from the midgut. These small RNAs hits were further searched in the host whole genome sequence to confirm that they are virus-borne. After excluding the hits mapped on to the host genome, we got 19 BmNPV-encoded small RNA sequences (14 from the fat body and 5 from the midgut). These small RNAs were subsequently scanned for the characteristic stem-loop structure of miRNA precursors (pre-miRNAs), which distinguish them from other small RNAs, particularly siRNAs (Ambros et al., 2003). The precursor sequences of all the 19 small RNAs were extracted by taking sequences flanking to these small RNAs into consideration, and their secondary structures were determined by MFold program (Zuker and Stiegler, 1981). MFold calculates minimum free energy (MFE) (Wuchty et al., 1999) for all the possible secondary structures of a given primary sequence. Finally, only 5 small RNAs (3 from the fat body and 2 from the midgut) could meet the criteria prescribed for miRNAs based on the MFE (<—20 kcal/mol) and the position of the matured miRNA on the stem-loop structured pre-miRNA (Ambros et al., 2003). Details of these 5 virus-encoded miRNAs and their pre-miRNAs are given in Tables 1 and S1 (supplementary file1) respectively, and their stem-loop secondary structures are shown in Fig. 2. Besides, we have predicted hundreds of host miRNAs with copy numbers ranging from 1 (*bmo-miR-308*) to 5779 (*bmo-miR-8*). Some of the known host miRNAs and their richness are listed in supplementary Table S3. Naming of the predicted miRNAs was done in accordance with the miRBase database. The mature sequences are designated as 'miR', and the precursor sequences as "mir" with the prefix "*bmnpv*" for BmNPV.

All the 5 BmNPV pre-miRNA locations were found to be oriented in the same direction and were confined within the 25 kb (80268–105117) region in the BmNPV genome suggesting that all these miRNAs are possibly derived from a single pri-miRNA transcript (supplementary Fig. S2). Two of the miRNAs i.e. *bmnpv-mir-1* and *bmnpv-mir-5* were encoded within the open reading frame (ORF) of viral cathepsin (AY817140) and alkaline nuclease (DQ263225), respectively. On the other hand, *bmnpv-mir-2* and *bmnpv-mir-3* were transcribed from the opposite strands of the chitinase (AY835395) and DNA-binding protein (M63416) ORFs, respectively. Whereas, *bmnpv-mir-4* was found to be transcribed from an unknown ORF. Similar observations have also been reported for many of the

Table 1
Genomic position, sequence and experimental validation of BmNPV-encoded miRNAs.

miRNA	Length	Genomic Location		Experimental validation	Sequence
bmnpv-miR-1	21	99318	99338	Validated	AAAUGGGCGGCGUACAGCUGG
bmnpv-miR-2	21	98020	98040	Validated	GGGGUUUUUGUACGGCGGCCC
bmnpv-miR-3	22	80278	80299	Validated	GAAAGCCAAACGAGGGCAGGCG
bmnpv-miR-4	23	83308	83330	Validated	GGUGGAUGUGAUUGUUGACGACA
bmnpv-miR-5	20	105077	105096	No	ACUAUAGUGGUCAAGAAAUC

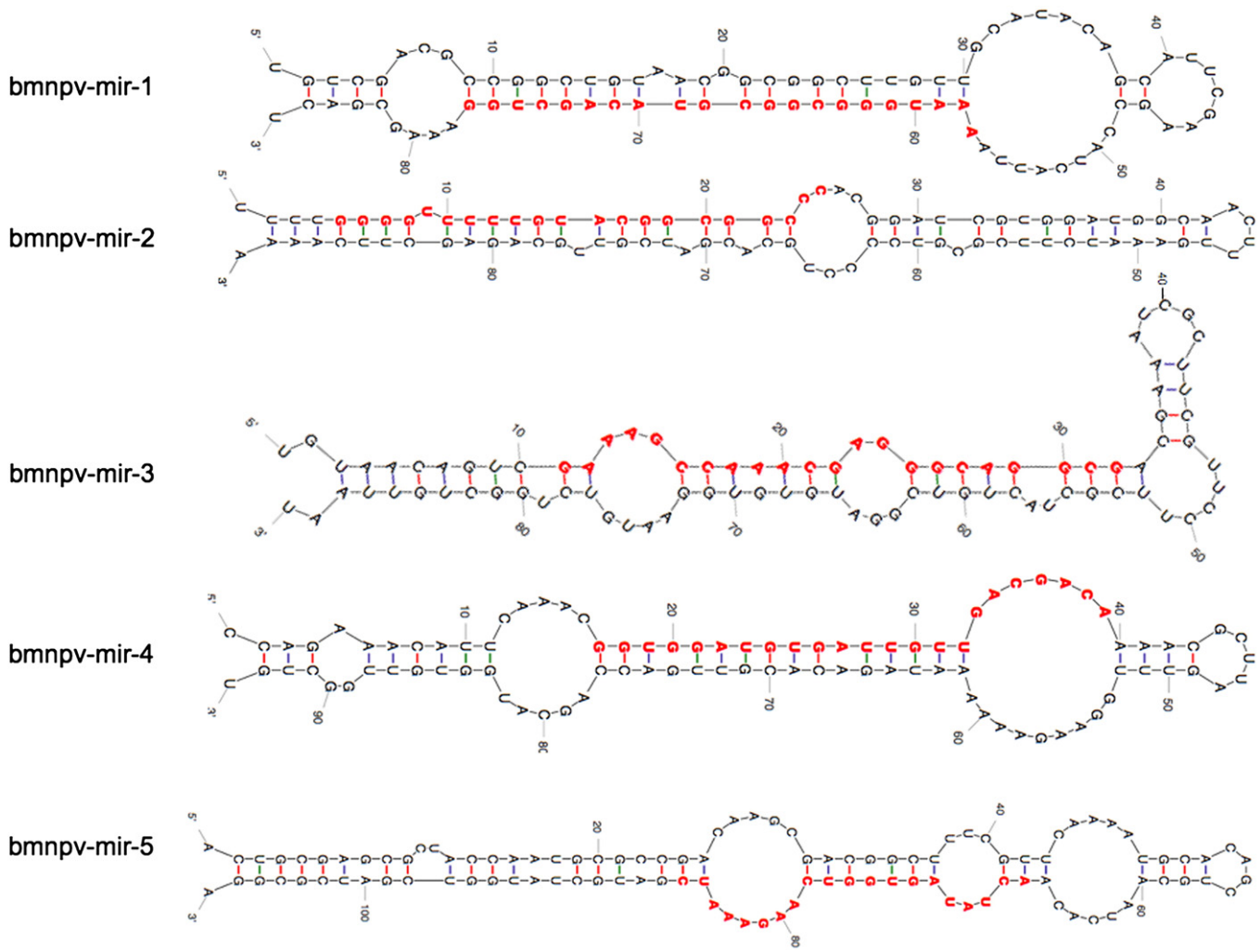

Fig. 2. Secondary structures of predicted viral miRNA precursors produced by Mfold program. The matured miRNA sequences are highlighted in red.

viral miRNAs, and it is reasoned that due to size constraint, viral genomes tend to consist of many overlapping ORFs (Cai et al., 2006; Pfeffer et al., 2004; Umbach et al., 2008).

Expression validation of predicted viral miRNAs

We have used three different techniques for validation of expression of these predicted miRNAs because the frequency of each miRNA recovered from deep sequencing of RNA harvested from tissues was very low (Table S4 of supplementary file1). One of the possible reasons for low abundance of miRNAs reported in the present study could be that we have extracted the RNA from tissues infected *in vivo* instead of viral-infected cell lines, which generally give high virus titre and hence higher frequency of virus-encoded miRNAs.

Northern blot Hybridization

We carried out Northern blot hybridization using RNAs from both infected and uninfected fat body and midgut tissues. Antisense oligonucleotides specific to each predicted BmNPV miRNA were end-labeled to high specific activity with [γ^{-32}P] ATP. No hybridizing species were detected in RNA harvested from either of the uninfected tissues (data not shown). However, positive signals were observed in RNA harvested from both the infected samples. In contrast to our sequencing analyses that recovered *bmnpv-miR-1, bmnpv-miR-2* and *bmnpv-miR-3* only from the infected fat body and *bmnpv-miR-4, bmnpv-miR-5* only from the infected midgut, we found expression of these miRNAs in both the infected tissues (Fig. 3) although level of expression of *bmnpv-miR-1, bmnpv-miR-2, bmnpv-miR-3* in the infected midgut tissue was very low as compared to the infected fat body. A 90 nucleotides long premiRNA expression was also detected in case of *bmnpv-miR-3.* Moreover, no positive signal specific to *bmnpv-miR-5* was detected in either of the infected tissues (data not shown). Detection of these miRNAs in Northern blot clearly indicates that the number of reads of each miRNA represented in the sequencing data is just a subset of the actual population in the cell. The expression results were further confirmed by stem-loop RT-PCR and Poly(A)-tailed RT-PCR.

Stem–loop RT-PCR

Less abundant miRNAs generally escape detection with standard methods such as northern hybridization (Lim et al., 2003) and microarray analysis (Liu et al., 2004). Stem-loop RT-PCR has proved to be very sensitive and can even discriminate among related miRNAs, which differ by as little as one nucleotide (Chen et al., 2005; Ro et al., 2006; Varkonyi-Gasic et al., 2007; Yu et al., 2008). Expression analysis of all the five miRNAs was carried out using infected and uninfected (control) fat body and midgut RNA samples. cDNA was prepared using stem-loop RT primer and then the RT product was amplified using a miRNA-specific forward primer and the universal reverse primer as described in Materials and methods. The expected length of the miRNA-amplified product was approximately 63 bp (see the

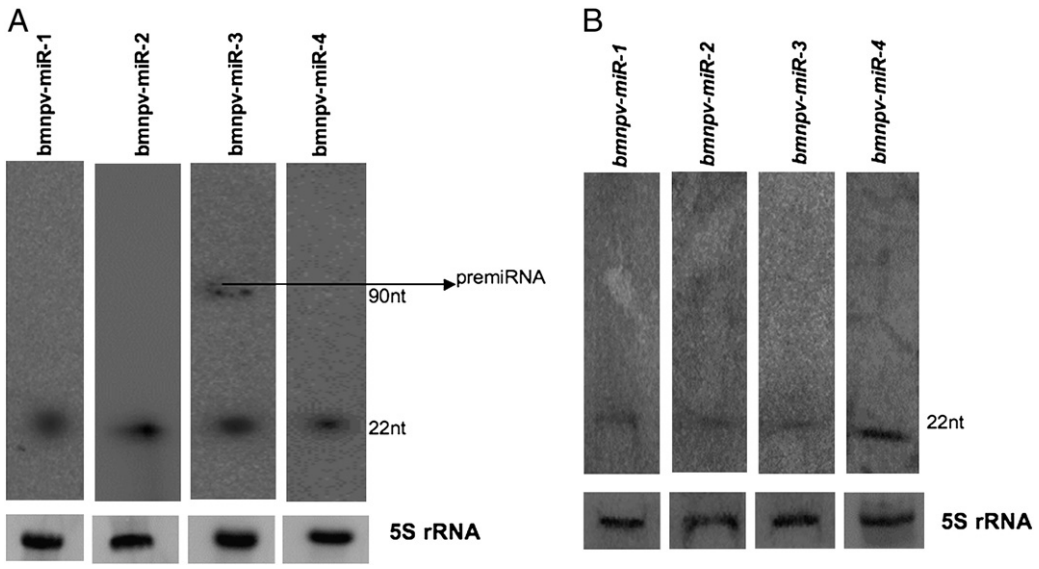

Fig. 3. Northern blot confirmation of predicted BmNPV-encoded miRNAs expression. (A) Northern blot analysis of small RNA samples derived from infected fat body tissue. Lane 1: *bmnpv-miR-1;* lane 2: *bmnpv-miR-2*; lane 3: *bmnpv-miR-3*; lane 4: *bmnpv-miR-4*. (B) Northern blot analysis of small RNA sample derived from infected midgut. Lane 1: *bmnpv-miR-1*; lane 2: *bmnpv-miR-2*; lane 3: *bmnpv-miR-3*; lane 4: *bmnpv-miR-4*. 5S rRNA was used as a loading control.

supplementary file1 for the product size calculation). The amplified PCR products were then detected on 4% agarose gel with EtBr staining.

Stem-loop RT-PCR results were consistent with the Northern blot analyses; *bmnpv-miR-1, bmnpv-miR-2, bmnpv-miR-3* and *bmnpv-miR-4* were found to be expressed in both the infected tissues (Fig. 4A and B). The PCR products of stem-loop PCR were cloned and sequenced to exclude any chance of getting a non-specific product (like primer-dimer or other artifacts) of expected size. Again, we did not observe expression of *bmnpv-miR-5* in either of the infected tissues.

Poly(A)-tailed RT-PCR

The cDNAs were prepared as described in Materials and methods, and then the polyadenylated cDNAs were amplified by PCR using

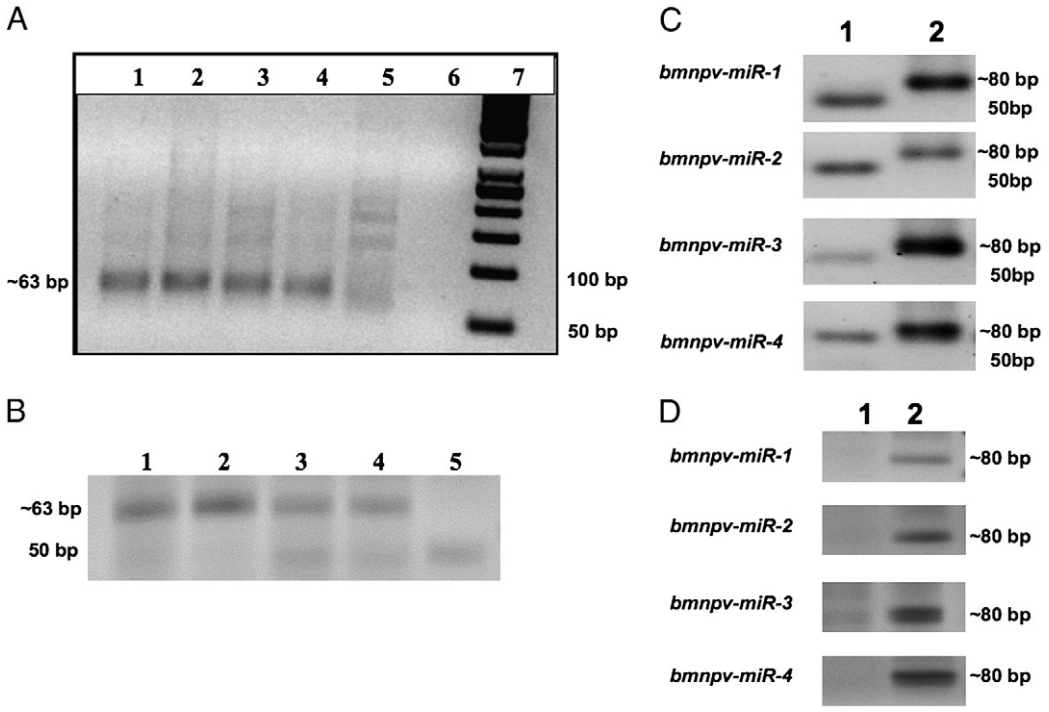

Fig. 4. Expression of predicted viral miRNAs investigated by stem-loop RT-PCR and poly(A)-tailed RT-PCR. (A) Stem-loop RT-PCR analyses of 5 predicted BmNPV-encoded miRNAs in infected fat body. Lane 1: *bmnpv-miR-1*; lane 2: *bmnpv-miR-2*; lane 3: *bmnpv-miR-3*; lane 4: *bmnpv-miR-4*; lane 5: *bmnpv-miR-5*; lane 6: minus RT control; lane 7: 50 bp DNA ladder. (B) Stem-loop RT-PCR analyses of 5 predicted BmNPV-encoded miRNAs in infected midgut. Lane 1: *bmnpv-miR-1*; lane 2: *bmnpv-miR-2*; lane 3: *bmnpv-miR-3*; lane 4: *bmnpv-miR-4*; lane 5: *bmnpv-miR-5*; lane 6: minus RT control. **C.** Reconfirmation of expression of *bmnpv-miR-1, bmnpv-miR-2, bmnpv-miR-3 and bmnpv-miR-4* in the infected fat body tissue by poly (A)-tailed RT-PCR. Lane 1: control fat body RNA; lane 2: Infected fat body RNA. (D) Poly (A)-tailed RT-PCR analyses of *bmnpv-miR-1, bmnpv-miR-2, bmnpv-miR-3 and bmnpv-miR-4* expression in infected midgut tissue. Lane 1: control midgut RNA; lane 2: Infected midgut RNA. 10 μl of PCR product was used in all the experiments and the 50 bp PCR product is a primer-dimer.

miRNA specific forward and universal reverse primers. The PCR products were resolved on 4% agarose gels with EtBr and visualized under UV light. Again, we got results similar to Northern blot and stem-loop RT-PCR analyses, bands of expected length (~80 bp) for *bmnpv-miR-1, bmnpv-miR-2, bmnpv-miR-3* and *bmnpv-miR-4* (see Fig. 4C and D) were seen in both the infected tissues. All the miRNA sequences were further confirmed by cloning followed by sequencing of the PCR products. Since we did not observe expression of *bmnpv-miR-5* by any of the methods, we retained only the 4 validated viral miRNAs for further analysis.

Conservation of BmNPV miRNAs

Evolutionary relationships based on whole genome sequence data are well studied in Baculoviruses (Herniou et al., 2001, 2003, 2004). According to the recent phylogeny (Goodman et al., 2007), BmNPV belongs to group 1 of Nucleopolyhedrosis viruses and shares the clade with *Autographa californica* nucleopolyhedrovirus (AcMNPV), *Bombyx mandarina* nucleopolyhedrovirus (BomaNPV), *Plutella xylostella* multiple nucleopolyhedrovirus (PxMNPV), *Rachiplusia ou* multiple nucleopolyhedrovirus (RoMNPV) and *Maruca vitrata* multiple nucleopolyhedrovirus (MaviNPV). Given the similarity between these genomes, it was interesting to look for the conservation of viral miRNAs among these viruses. A recent report on global analysis of evolutionary conservation among the miRNAs encoded by Gammaherpesviruses (maximum number of miRNAs is reported from this group of viruses) indicates a high degree of conservation at the genomic locations, but sequences were found to be quite unrelated (Walz et al., 2009). However, we found that all the four BmNPV miRNAs that we have identified in the present study are remarkably conserved in AcMNPV, BomaNPV and PxMNPV, being 100% identical. Whereas, three miRNAs are conserved in RoMNPV and one in MaviNPV (A descriptive detail is given in supplementary file3). Although the sequences of the predicted precursors were not well conserved, all of them were able to make typical hairpin structure and also passed our other criteria of hairpin-like secondary structure. Conservation of these miRNAs clearly implies that viral miRNAs are under strong selection pressure and play potentially critical role in viral life cycle. Recently, many reports have also suggested that viral miRNAs share seed region homology with host miRNAs to hijack the host defense machinery (Gottwein et al., 2007; Skalsky et al., 2007) but when we carried out similar analyses, we could not find any seed homology between BmNPV and the known *B. mori* miRNAs. Further, we also performed a seed homology search of these miRNAs against all the known miRNAs reported in miRbase (Release 14) from different species. Though we got hits for *bmnpv-miR-2*, *bmnpv-miR-3* and *bmnpv-miR-4* in other miRNAs of unrelated species (supplementary Fig. S3), none of these miRNAs were found to be conserved in the *B. mori* genome.

Target prediction

Viruses employ miRNAs to regulate both cellular and their own gene expression in order to modulate the antiviral host defense machinery for eventual invasion and proliferation inside the host (Barth et al., 2008; Bennasser et al., 2004; Murphy et al., 2008; Samols et al., 2007). Primarily, miRNA binds to 3′ UTR (Brennecke et al., 2003; Lin et al., 2003) of the target mRNA but many recent reports suggest that miRNAs also bind to 5′UTR (Lytle et al., 2007) or coding sequence (CDS) (Forman et al., 2008; Nielsen et al., 2009), and repress the expression of target mRNAs with similar efficiency. Taking these reports into consideration, we examined the full-length mRNA sequences of virus and host for the prediction of viral miRNA targets. We first used miRanda target prediction program, which is based on dynamic-programming alignments and many statistical parameters. Results were then screened using different filters to enhance the specificity of the program thus ensuring the least false positives. An overview of different steps that were followed in target prediction is shown in Fig. 5.

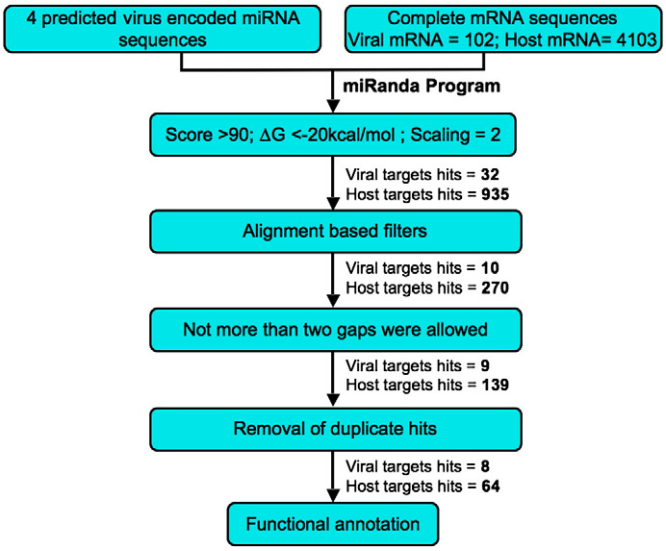

Fig. 5. An overview of different steps and filters involved in target prediction of BmNPV-encoded miRNAs.

We found 32 viral and 935 cellular target hits after the first filter; these hits were then scanned for consecutive Watson-Crick matches on the position 2 to 8 at the 5′ end of a miRNA i.e. *seed region* (Krek et al., 2005; Lewis et al., 2005). To increase the sensitivity of the program a single G:U pairing was allowed in the seed region as G:U pairing is also tolerable in various positions of the *seed region* (Didiano and Hobert, 2006). Base pairing of the miRNA at 3′end and minimum gaps were also taken into account for strengthening the miRNA::mRNA alignment (Enright et al., 2003). Finally, removal of duplicate entries yielded 8 viral and 64 cellular target hits for viral miRNAs. Details of all the predicted targets are shown in the supplementary file3. MicroRNAs *bmnpv-miR-1* and *bmnpv-miR-4* were found to have maximum viral and cellular target hits respectively (Table S7 of supplementary file1). Interestingly, two of the predicted viral targets (DNA-binding protein and viral chitinase) were found to be targeted by miRNAs, which transcribed from the regions that are exactly opposite to their own locations on the genome (see Table 2). Such examples have been reported previously from many viruses (Barth et al., 2008; Sullivan and Ganem, 2005a; Tang et al., 2008; Umbach et al., 2008).

Functions of viral targets

Virus-encoded miRNA regulation of viral replication is a general phenomenon as suggested by earlier reports (Barth et al., 2008; Hussain et al., 2008). Our target prediction is consistent with these reports, as we have found target hits on the three very important components of viral replication machinery i.e. DNA-binding protein, DNA helicase and DNA polymerase (Table 2).

BmNPV displays a biphasic intracellular localization during infection. Initially, it multiples inside the nucleus and then in later stages it localizes in the cytoplasm and hence, clearly implies the importance of nuclear export pathway during infection. We have found the target hit of *bmnpv-miR-1* and *bmnpv-miR-3* on bro-I and bro-III (baculovirus repeat ORF) genes respectively, which are known to be involved in viral nuclear export pathway (Kang et al., 2006) and are conserved in many other dsDNA insect viruses like ascoviruses (Bideshi et al., 2003) and iridovirus (Jakob et al., 2001). The other candidate target genes of interest were fusolin (gp37-BmORF-52 = AcORF64) and *lef-8* (late expressing factor). Fusolin is known to strongly enhance the peroral infectivity of several insect viruses

Table 2
The predicted viral targets of BmNPV-encoded miRNAs and their molecular functions.

Accession No.	miRNA(s) hit	miRNA binding site on mRNA	MFE (Kcal/mol)	Known function
M63416	*bmnpv-miR-3*	458–479 (3′UTR)	−48.48	DNA-binding protein.
AY835395	*bmnpv-miR-2*	668–688 (CDS)	−47.48	Virus K1 chitinase gene.
5AJ309235	*bmnpv-miR-1*	912–932 (CDS)	−29.83	Virus bro-I gene.
AY449788	*bmnpv-miR-4*	369–390 (CDS)	−30.58	Virus *lef-8* gene.
AJ309237	*bmnpv-miR-3*	521–540 (CDS)	−24.49	Virus bro-III gene.
U55071	*bmnpv-miR-1*	1628–1647 (3′UTR)	−20.19	Virus fusolin gene.
D16231	*bmnpv-miR-1*	806–826 (CDS)	−22.97	Virus DNA polymerase.
Y10101	*bmnpv-miR-4*	1164–1183 (CDS)	−24.61	Viral gene encoding p25, putative helicase and ORF3.

(Takemoto et al., 2008) and *lef-8*, along with other factors, constitute the primary components of RNA polymerase, which is essential for the initiation of transcription from late and very late promoters (Acharya and Gopinathan, 2002). Additional details of viral targets are given in supplementary file 3.

Functions of cellular-targets

We have predicted a number of interesting cellular targets that are involved in different antiviral host defense mechanisms (see Table 3); a few of them are discussed here.

In insect system, the humoral response is mainly characterized by rapid activation of prophenoloxidase cascade, which results in the limited proteolysis of the zymogenic prophenoloxidase to active phenoloxidase by serine proteases (Cerenius and Soderhall, 2004; Satoh et al., 1999). Similarly, recognition of viral infection by Lepidopteran-specific pattern recognition proteins like hemolin is an essential step of host immune defense (Terenius, 2008). Hemolin is known to mediate many other anti-viral activities like hemocyte aggregation, nodule formation and phagocytosis (Eleftherianos et al., 2007).

The other important targets were GTP-binding nuclear protein Ran, DEAD box polypeptides and eukaryotic translation initiation factors, which play a decisive role in small RNA mediated gene regulation. Ran-GTP acts as a cofactor for Exportin-5, which governs the nuclear export of pre-miRNA from nucleus to the cytoplasm. Exportin-5 binds to pre-miRNA in the presence of Ran-GTP, whereas, hydrolysis of Ran-GTP to Ran-GDP is essential for the release of pre-miRNA in the cytoplasm (Yi et al., 2003). DEAD-box proteins are important for the helicase and transcriptional repression activities of small non-coding RNAs mediated gene-regulation (Tabara et al., 2002; Yan et al., 2003). Similarly, inhibition of eukaryotic initiation factor 4E, a 5′cap-binding protein, is known to be an essential step in controlling the translation initiation by miRNAs (Humphreys et al., 2005).

The computationally identified targets in the present study suggest that virus-encoded miRNAs probably have important role in regulating a range of cellular activities for easy establishment of the virus in the host. The studies are now underway in our lab to validate these targets and their function(s).

Our increasing knowledge of the host–virus interaction at the molecular level should lead us towards the possible explanation for viral tropism, latency and counter host response, which will help in development of an effective, durable and nontoxic antiviral therapy using miRNAs. The different silkworm strains available in silkworm germplasm collections show a great degree of variation with regards to their resistance/susceptibility to BmNPV infection. Hence, the present study on identification of viral miRNAs and their targets would also allow us to understand the possible role of miRNA(s) mediated resistance/susceptibility in silkworm against baculovirus infection.

Materials and methods

B. mori and BmNPV infection

The silkworm, *B. mori* strain SBNP-1 was provided by Andhra Pradesh State Sericulture Research and Development Institute (APSSRDI), Hindupur, India. The larvae were reared at 27 °C on fresh mulberry leaves. Freshly eclosed fifth instar larvae were orally fed with purified BmNPV suspension of occlusion bodies (OBs) (20,000OBs/larva).

Collection of tissues

The fat body and midgut tissues were extracted from BmNPV-infected larvae at 48 hours of post infection, were washed in PBS solution (137 mM NaCl, 2.68 mM KCl, 8.1 mM Na_2HPO_4, 1.47 mM KH_2PO_4 (pH 7.4)) prepared with diethylpyrocarbonate (DEPC) treated water and immediately snap frozen in liquid nitrogen.

RNA extraction and miRNA library preparation

Liquid nitrogen frozen tissues were homogenized in TRIzol reagent (Invitrogen®) and total RNA was extracted using standard protocol (http://www.animal.ufl.edu/hansen/Protocols/RNA_extraction.htm). cDNA library was developed based on the protocol described previously (Eveland et al., 2008). Briefly, small RNA molecules were isolated by size fractionation on a polyacrylamide gel; RNA adapters were sequentially ligated to the 3′ and 5′ ends; reverse transcriptase generated the first strand of cDNA followed by PCR amplification of the cDNA. Finally, size fractionation of the cDNA was done for GS FLX sequencing, developed by 454 Life Sciences® (Margulies et al., 2005).

Table 3
Cellular targets of BmNPV encoded miRNAs and their molecular functions.

Accession No.	miRNA(s) hit	miRNA binding site on mRNA	MFE (Kcal/mol)	Known function
DQ311402	*bmnpv-miR-1*	755–777 (3′UTR)	−23.82	GTP-binding nuclear protein Ran.
AB073673	*bmnpv-miR-1*	1174–1193 (CDS)	−23.34	Serine protease.
DQ443244	*bmnpv-miR-2*	347–367 (CDS)	−25.49	Eukaryotic translation initiation factor 4E-binding protein.
AB115084	*bmnpv-miR-2*	442 462 (CDS)	−22.81	*Bombyx mori* Hemolin.
D49371	*bmnpv-miR-3*	2646–2669 (3′UTR)	−23.21	Prophenoloxidase.
DQ443284	*bmnpv-miR-4*	894–915 (CDS)	−28.1	Chymotrypsin-like serine protease.
AB026260	*bmnpv-miR-4*	1059–1081 (CDS)	−20.28	Cadherin-like membrane protein.
DQ443223	*bmnpv-miR-4*	1543–1566 (CDS)	−29.75	DEAD box polypeptide.

Bioinformatic data analysis pipeline

Viral and host genomes were downloaded from NCBI (http://www.ncbi.nlm.nih.gov/) with GenBank: Accession no. L33180, and SilkDB (http://silkworm.genomics.org.cn) respectively. Around 70,000 sequenced reads of 19–26 nucleotides from both the infected tissues were mapped on to the viral genome using BLASTn with *e*-value<0.1; identity≥18 nucleotides and mismatches≤2. The rest of the parameters including low complexity filter were taken as default. The selected hits were then searched against the host genome using BLASTn with the same parameters and all the mapped hits, which were showing identity score higher than on the viral genome were removed from the list of potential miRNAs to ensure the retention of only viral borne miRNAs.

Secondary structure of pre-miRNAs

The precursor sequences of predicted miRNAs were extracted by taking flanking sequences of mature miRNA into consideration. A sliding window of size ~100 nt (moving in the increment of ~10 nt) was taken from the region ~80 nt upstream of the beginning of the mature miRNA to ~80 nt downstream of the miRNA (Singh and Nagaraju, 2008). The extracted pre-miRNA sequences were then submitted to Mfold program for predicting their secondary structure (s). Selection of pre-miRNA structures was based on the following criteria: (a) Free energy change (ΔG) less than −20 kcal/mole and b) Mature miRNA sequences should not be on the loop region (variable region) of the hairpin.

Northern blot analysis

Small RNAs (<200 nt) were isolated from both infected and control tissues using the *mir*Vana miRNA Isolation kit according to the manufacturer's protocol (Ambion, Austin, TX), and Northern blot analysis was done as previously described (Cai et al., 2006). Briefly, 10 μg of each small RNA fraction, as well as radiolabeled Decade Markers (Ambion), were separated on 15% denaturing polyacrylamide gel electrophoresis (PAGE) (acrylamide:bis-acrylamide ratio, 19:1). RNAs were then transferred to a positively charged nylon membrane (Zeta-probe GT membrane, Bio-Rad) using Semi-dry transfer cell (Trans-blot® SD Bio-Rad) and UV cross-linked to the membrane.

Probe preparation

The reverse complementary DNA probes of the five predicted viral miRNAs (supplementary file1 Table S5) were end labeled with [γ^{-32}P] ATP (specific activity $>1\times10^8$ cpm/pmol) using T4-polynucleotide Kinase (T4 PNK, TAKARA). The labeled probes were then purified using MicroSpin™ G-25 Columns (GE Healthcare), according to the manufacturer's protocols. Hybridizations and washes were carried out using the ULTRAhyb-Oligo hybridization buffer and wash solutions from Northern Max™ kit (Ambion), and signals were detected by phosphor imager FLA-9000 Starion (Fujifilm Global).

Stem-loop RT-PCR confirmation

All the stem-loop RT-PCR primers are listed in Table S6 of supplementary file1.

RT reaction

cDNA was synthesized from the small RNA by using 8 nucleotides miRNA specific stem-loop primers as previously described (Yu et al., 2008), with some modifications. The 20 μl reverse transcription reaction included 3 μg RNA, 1 μl 10 mM dNTPs (Fermentas®) and 1 μl 50nM stem-loop primer. The reaction mixture was heated at 65 °C for 5 min and then immediately placed on ice. The contents were collected by brief centrifugation and then 4 μl 5× first strand buffer (Invitrogen®), 1 μl 0.1 M DTT and 1 μl 200U/μl Superscript III reverse transcriptase (Invitrogen®) were added and this mixture was incubated at 55 °C for 60 min. The reverse transcriptase enzyme was finally inactivated at 70 °C for 15 min.

PCR reaction

20 μl PCR mixture contained 1.5 μl cDNA, 2 μl 10× PCR buffer, 0.2 μl 10 mM dNTPs (Fermentas®), 1.2 μl 25 mM $MgCl_2$, 1 μl each of 5 μM forward and reverse primers, 0.2 μl 5U/μl Taq polymerase (Fermentas®) and nuclease-free water to make up the volume. PCR reaction was performed using Applied Biosystems® Gene Amp 9700 Thermal Cycler in 200 μl micro-tubes for 3 min at 95 °C, followed by 35 cycles of 30 sec at 95 °C, 30 s at 60 °C, 1 min at 72 °C and final extension at 72 °C for 7 min. 10 μl of PCR products were resolved on a 4% agarose gel electrophoresis containing ethidium bromide and photographed under UV light.

Poly(A)-tailed RT-PCR

Poly(A)-tailed RT-PCR (17) was done using NCode miRNA First strand cDNA synthesis and qRT-PCR Kits (Invitrogen®) as per manufacturer's protocol. The schematic of the whole procedure is given in Fig. S1 of supplementary material.

Sequencing of PCR product

Cloning of PCR products was done by using TOPO TA Cloning System (Invitrogen®) based on manufacturer's protocol. The inserted PCR product sequence was determined using ABI PRISM® 3100 Genetic Analyzer.

Target prediction using miRanda program

A total of 4103 mRNA sequences of *B. mori* was downloaded from NCBI database and searched for potential targets of the predicted virus miRNAs using miRanda. The parameters assigned for miRanda were Smith-Waterman hybridization alignment score greater than 90 (Smith and Waterman, 1981), ΔG of miRNA::mRNA duplex less than −20 kcal/mol, scaling factor equal 2, and the other parameters were kept as default.

Screening of Target hits

Screening of miRNA-target alignments was based on the following four empirical rules (position count starting from 5′ end of the miRNA): a) no mismatches at positions 2 to 8 (seed region), b) not more than one G:U pairing allowed in the seed region, c) at least 2 matches should be there in the last five positions of the alignment, and d) not more than two gaps were allowed in the alignment.

Supplementary materials related to this article can be found online at doi:10.1016/j.virol.2010.07.033.

Acknowledgments

JN acknowledges financial support from the Department of Biotechnology, Government of India under Centre of Excellence for Genetics and Genomics of Silkmoths. JS is the recipient of a senior research fellowship from the Department of Biotechnology, Government of India and CPS is the recipient of senior research fellowship from the Council of Scientific and Industrial Research, India.

References

Acharya, A., Gopinathan, K.P., 2002. Characterization of late gene expression factors lef-9 and lef-8 from *Bombyx mori* nucleopolyhedrovirus. J. Gen. Virol. 83 (Pt 8), 2015–2023.

Altschul, S.F., Gish, W., Miller, W., Myers, E.W., Lipman, D.J., 1990. Basic local alignment search tool. J. Mol. Biol. 215 (3), 403–410.

Ambros, V., Bartel, B., Bartel, D.P., Burge, C.B., Carrington, J.C., Chen, X., Dreyfuss, G., Eddy, S.R., Griffiths-Jones, S., Marshall, M., Matzke, M., Ruvkun, G., Tuschl, T., 2003. A uniform system for microRNA annotation. RNA 9 (3), 277–279.

Bartel, D.P., 2004. MicroRNAs: genomics, biogenesis, mechanism, and function. Cell 116 (2), 281–297.

Barth, S., Pfuhl, T., Mamiani, A., Ehses, C., Roemer, K., Kremmer, E., Jaker, C., Hock, J., Meister, G., Grasser, F.A., 2008. Epstein–Barr virus-encoded microRNA miR-BART2 down-regulates the viral DNA polymerase BALF5. Nucleic Acids Res. 36 (2), 666–675.

Bennasser, Y., Le, S.Y., Yeung, M.L., Jeang, K.T., 2004. HIV-1 encoded candidate micro-RNAs and their cellular targets. Retrovirology 1, 43.

Bideshi, D.K., Renault, S., Stasiak, K., Federici, B.A., Bigot, Y., 2003. Phylogenetic analysis and possible function of bro-like genes, a multigene family widespread among large double-stranded DNA viruses of invertebrates and bacteria. J. Gen. Virol. 84 (Pt 9), 2531–2544.

Brennecke, J., Hipfner, D.R., Stark, A., Russell, R.B., Cohen, S.M., 2003. bantam encodes a developmentally regulated microRNA that controls cell proliferation and regulates the proapoptotic gene hid in Drosophila. Cell 113 (1), 25–36.

Bulet, P., Stocklin, R., Menin, L., 2004. Anti-microbial peptides: from invertebrates to vertebrates. Immunol. Rev. 198, 169–184.

Cai, X., Lu, S., Zhang, Z., Gonzalez, C.M., Damania, B., Cullen, B.R., 2005. Kaposi's sarcoma-associated herpesvirus expresses an array of viral microRNAs in latently infected cells. Proc. Natl. Acad. Sci. U. S. A. 102 (15), 5570–5575.

Cai, X., Schafer, A., Lu, S., Bilello, J.P., Desrosiers, R.C., Edwards, R., Raab-Traub, N., Cullen, B.R., 2006. Epstein–Barr virus microRNAs are evolutionarily conserved and differentially expressed. PLoS Pathog. 2 (3), e23.

Cerenius, L., Soderhall, K., 2004. The prophenoloxidase-activating system in invertebrates. Immunol. Rev. 198, 116–126.

Chen, C., Ridzon, D.A., Broomer, A.J., Zhou, Z., Lee, D.H., Nguyen, J.T., Barbisin, M., Xu, N. L., Mahuvakar, V.R., Andersen, M.R., Lao, K.Q., Livak, K.J., Guegler, K.J., 2005. Real-time quantification of microRNAs by stem-loop RT-PCR. Nucleic Acids Res. 33 (20), e179.

Didiano, D., Hobert, O., 2006. Perfect seed pairing is not a generally reliable predictor for miRNA-target interactions. Nat. Struct. Mol. Biol. 13 (9), 849–851.

Eleftherianos, I., Gokcen, F., Felfoldi, G., Millichap, P.J., Trenczek, T.E., Ffrench-Constant, R.H., Reynolds, S.E., 2007. The immunoglobulin family protein Hemolin mediates cellular immune responses to bacteria in the insect *Manduca sexta*. Cell. Microbiol. 9 (5), 1137–1147.

Enright, A.J., John, B., Gaul, U., Tuschl, T., Sander, C., Marks, D.S., 2003. MicroRNA targets in Drosophila. Genome Biol. 5 (1), R1.

Eveland, A.L., McCarty, D.R., Koch, K.E., 2008. Transcript profiling by 3′-untranslated region sequencing resolves expression of gene families. Plant Physiol. 146 (1), 32–44.

Forman, J.J., Legesse-Miller, A., Coller, H.A., 2008. A search for conserved sequences in coding regions reveals that the let-7 microRNA targets Dicer within its coding sequence. Proc. Natl. Acad. Sci. U. S. A. 105 (39), 14879–14884.

Fu, H.J., Zhu, J., Yang, M., Zhang, Z.Y., Tie, Y., Jiang, H., Sun, Z.X., Zheng, X.F., 2006. A novel method to monitor the expression of microRNAs. Mol. Biotechnol. 32 (3), 197–204.

Goodman, D., Ollikainen, N., Sholley, C., 2007. Baculovirus phylogeny based on genome rearrangements. In: Tesler, G., Durand, D. (Eds.), Comparative Genomics. International Workshop, RECOMB-CG 2007, San Diego, CA, USA, pp. 69–82.

Gottwein, E., Mukherjee, N., Sachse, C., Frenzel, C., Majoros, W.H., Chi, J.T., Braich, R., Manoharan, M., Soutschek, J., Ohler, U., Cullen, B.R., 2007. A viral microRNA functions as an orthologue of cellular miR-155. Nature 450 (7172), 1096–1099.

Griffiths-Jones, S., 2004. The microRNA Registry. Nucleic Acids Res. 32 (Database issue), D109–11.

Grishok, A., Pasquinelli, A.E., Conte, D., Li, N., Parrish, S., Ha, I., Baillie, D.L., Fire, A., Ruvkun, G., Mello, C.C., 2001. Genes and mechanisms related to RNA interference regulate expression of the small temporal RNAs that control *C. elegans* developmental timing. Cell 106 (1), 23–34.

Gupta, A., Gartner, J.J., Sethupathy, P., Hatzigeorgiou, A.G., Fraser, N.W., 2006. Anti-apoptotic function of a microRNA encoded by the HSV-1 latency-associated transcript. Nature 442 (7098), 82–85.

Herniou, E.A., Luque, T., Chen, X., Vlak, J.M., Winstanley, D., Cory, J.S., O'Reilly, D.R., 2001. Use of whole genome sequence data to infer baculovirus phylogeny. J. Virol. 75 (17), 8117–8126.

Herniou, E.A., Olszewski, J.A., Cory, J.S., O'Reilly, D.R., 2003. The genome sequence and evolution of baculoviruses. Annu. Rev. Entomol. 48, 211–234.

Herniou, E.A., Olszewski, J.A., O'Reilly, D.R., Cory, J.S., 2004. Ancient coevolution of baculoviruses and their insect hosts. J. Virol. 78 (7), 3244–3251.

Hultmark, D., Steiner, H., Rasmuson, T., Boman, H.G., 1980. Insect immunity. Purification and properties of three inducible bactericidal proteins from hemolymph of immunized pupae of *Hyalophora cecropia*. Eur. J. Biochem. 106 (1), 7–16.

Humphreys, D.T., Westman, B.J., Martin, D.I., Preiss, T., 2005. MicroRNAs control translation initiation by inhibiting eukaryotic initiation factor 4E/cap and poly(A) tail function. Proc. Natl. Acad. Sci. U. S. A. 102 (47), 16961–16966.

Hussain, M., Taft, R.J., Asgari, S., 2008. An insect virus-encoded microRNA regulates viral replication. J. Virol. 82 (18), 9164–9170.

Hutvagner, G., McLachlan, J., Pasquinelli, A.E., Balint, E., Tuschl, T., Zamore, P.D., 2001. A cellular function for the RNA-interference enzyme Dicer in the maturation of the let-7 small temporal RNA. Science 293 (5531), 834–838.

Jakob, N.J., Muller, K., Bahr, U., Darai, G., 2001. Analysis of the first complete DNA sequence of an invertebrate iridovirus: coding strategy of the genome of Chilo iridescent virus. Virology 286 (1), 182–196.

Kang, W., Kurihara, M., Matsumoto, S., 2006. The BRO proteins of *Bombyx mori* nucleopolyhedrovirus are nucleocytoplasmic shuttling proteins that utilize the CRM1-mediated nuclear export pathway. Virology 350 (1), 184–191.

Ketting, R.F., Fischer, S.E., Bernstein, E., Sijen, T., Hannon, G.J., Plasterk, R.H., 2001. Dicer functions in RNA interference and in synthesis of small RNA involved in developmental timing in *C. elegans*. Genes Dev. 15 (20), 2654–2659.

Krek, A., Grun, D., Poy, M.N., Wolf, R., Rosenberg, L., Epstein, E.J., MacMenamin, P., da Piedade, I., Gunsalus, K.C., Stoffel, M., Rajewsky, N., 2005. Combinatorial microRNA target predictions. Nat. Genet. 37 (5), 495–500.

Lau, N.C., Lim, L.P., Weinstein, E.G., Bartel, D.P., 2001. An abundant class of tiny RNAs with probable regulatory roles in *Caenorhabditis elegans*. Science 294 (5543), 858–862.

Lee, R.C., Feinbaum, R.L., Ambros, V., 1993. The *C. elegans* heterochronic gene lin-4 encodes small RNAs with antisense complementarity to lin-14. Cell 75 (5), 843–854.

Lee, Y., Jeon, K., Lee, J.T., Kim, S., Kim, V.N., 2002. MicroRNA maturation: stepwise processing and subcellular localization. EMBO J. 21 (17), 4663–4670.

Lee, Y., Ahn, C., Han, J., Choi, H., Kim, J., Yim, J., Lee, J., Provost, P., Radmark, O., Kim, S., Kim, V.N., 2003. The nuclear RNase III Drosha initiates microRNA processing. Nature 425 (6956), 415–419.

Lewis, B.P., Burge, C.B., Bartel, D.P., 2005. Conserved seed pairing, often flanked by adenosines, indicates that thousands of human genes are microRNA targets. Cell 120 (1), 15–20.

Lim, L.P., Glasner, M.E., Yekta, S., Burge, C.B., Bartel, D.P., 2003. Vertebrate microRNA genes. Science 299 (5612), 1540.

Lin, S.Y., Johnson, S.M., Abraham, M., Vella, M.C., Pasquinelli, A., Gamberi, C., Gottlieb, E., Slack, F.J., 2003. The *C. elegans* hunchback homolog, hbl-1, controls temporal patterning and is a probable microRNA target. Dev. Cell 4 (5), 639–650.

Liu, C.G., Calin, G.A., Meloon, B., Gamliel, N., Sevignani, C., Ferracin, M., Dumitru, C.D., Shimizu, M., Zupo, S., Dono, M., Alder, H., Bullrich, F., Negrini, M., Croce, C.M., 2004. An oligonucleotide microchip for genome-wide microRNA profiling in human and mouse tissues. Proc. Natl. Acad. Sci. U. S. A. 101 (26), 9740–9744.

Lytle, J.R., Yario, T.A., Steitz, J.A., 2007. Target mRNAs are repressed as efficiently by microRNA-binding sites in the 5′ UTR as in the 3′ UTR. Proc. Natl. Acad. Sci. U. S. A. 104 (23), 9667–9672.

Margulies, M., Egholm, M., Altman, W.E., Attiya, S., Bader, J.S., Bemben, L.A., Berka, J., Braverman, M.S., Chen, Y.J., Chen, Z., Dewell, S.B., Du, L., Fierro, J.M., Gomes, X.V., Godwin, B.C., He, W., Helgesen, S., Ho, C.H., Irzyk, G.P., Jando, S.C., Alenquer, M.L., Jarvie, T.P., Jirage, K.B., Kim, J.B., Knight, J.R., Lanza, J.R., Leamon, J.H., Lefkowitz, S.M., Lei, M., Li, J., Lohman, K.L., Lu, H., Makhijani, V.B., McDade, K.E., McKenna, M.P., Myers, E.W., Nickerson, E., Nobile, J.R., Plant, R., Puc, B.P., Ronan, M.T., Roth, G.T., Sarkis, G.J., Simons, J.F., Simpson, J.W., Srinivasan, M., Tartaro, K.R., Tomasz, A., Vogt, K.A., Volkmer, G.A., Wang, S.H., Wang, Y., Weiner, M.P., Yu, P., Begley, R.F., Rothberg, J.M., 2005. Genome sequencing in microfabricated high-density picolitre reactors. Nature 437 (7057), 376–380.

Murphy, E., Vanicek, J., Robins, H., Shenk, T., Levine, A.J., 2008. Suppression of immediate-early viral gene expression by herpesvirus-coded microRNAs: implications for latency. Proc. Natl. Acad. Sci. U. S. A. 105 (14), 5453–5458.

Nielsen, A.F., Gloggnitzer, J., Martinez, J., 2009. MicroRNAs cross the line: the battle for mRNA stability enters the coding sequence. Mol. Cell 35 (2), 139–140.

Pfeffer, S., Zavolan, M., Grasser, F.A., Chien, M., Russo, J.J., Ju, J., John, B., Enright, A.J., Marks, D., Sander, C., Tuschl, T., 2004. Identification of virus-encoded microRNAs. Science 304 (5671), 734–736.

Pfeffer, S., Sewer, A., Lagos-Quintana, M., Sheridan, R., Sander, C., Grasser, F.A., van Dyk, L.F., Ho, C.K., Shuman, S., Chien, M., Russo, J.J., Ju, J., Randall, G., Lindenbach, B.D., Rice, C.M., Simon, V., Ho, D.D., Zavolan, M., Tuschl, T., 2005. Identification of microRNAs of the herpesvirus family. Nat. Methods 2 (4), 269–276.

Reinhart, B.J., Slack, F.J., Basson, M., Pasquinelli, A.E., Bettinger, J.C., Rougvie, A.E., Horvitz, H.R., Ruvkun, G., 2000. The 21-nucleotide let-7 RNA regulates developmental timing in *Caenorhabditis elegans*. Nature 403 (6772), 901–906.

Ro, S., Park, C., Jin, J., Sanders, K.M., Yan, W., 2006. A PCR-based method for detection and quantification of small RNAs. Biochem. Biophys. Res. Commun. 351 (3), 756–763.

Rohrmann, G.F., 2008. Baculovirus Molecular Biology. National Library of Medicine (US), NCBI, Bethesda (MD).

Samols, M.A., Skalsky, R.L., Maldonado, A.M., Riva, A., Lopez, M.C., Baker, H.V., Renne, R., 2007. Identification of cellular genes targeted by KSHV-encoded microRNAs. PLoS Pathog. 3 (5), e65.

Satoh, D., Horii, A., Ochiai, M., Ashida, M., 1999. Prophenoloxidase-activating enzyme of the silkworm, *Bombyx mori*. Purification, characterization, and cDNA cloning. J. Biol. Chem. 274 (11), 7441–7453.

Schwarz, D.S., Tomari, Y., Zamore, P.D., 2004. The RNA-induced silencing complex is a Mg2+-dependent endonuclease. Curr. Biol. 14 (9), 787–791.

Singh, J., Nagaraju, J., 2008. In silico prediction and characterization of microRNAs from red flour beetle (*Tribolium castaneum*). Insect Mol. Biol. 17 (4), 427–436.

Skalsky, R.L., Samols, M.A., Plaisance, K.B., Boss, I.W., Riva, A., Lopez, M.C., Baker, H.V., Renne, R., 2007. Kaposi's sarcoma-associated herpesvirus encodes an ortholog of miR-155. J. Virol. 81 (23), 12836–12845.

Smith, T.F., Waterman, M.S., 1981. Identification of common molecular subsequences. J. Mol. Biol. 147 (1), 195–197.

Stark, A., Kheradpour, P., Parts, L., Brennecke, J., Hodges, E., Hannon, G.J., Kellis, M., 2007a. Systematic discovery and characterization of fly microRNAs using 12 Drosophila genomes. Genome Res. 17 (12), 1865–1879.

Stark, A., Lin, M.F., Kheradpour, P., Pedersen, J.S., Parts, L., Carlson, J.W., Crosby, M.A., Rasmussen, M.D., Roy, S., Deoras, A.N., Ruby, J.G., Brennecke, J., Hodges, E., Hinrichs, A.S., Caspi, A., Paten, B., Park, S.W., Han, M.V., Maeder, M.L., Polansky, B.J., Robson, B. E., Aerts, S., van Helden, J., Hassan, B., Gilbert, D.G., Eastman, D.A., Rice, M., Weir, M.,

Hahn, M.W., Park, Y., Dewey, C.N., Pachter, L., Kent, W.J., Haussler, D., Lai, E.C., Bartel, D.P., Hannon, G.J., Kaufman, T.C., Eisen, M.B., Clark, A.G., Smith, D., Celniker, S.E., Gelbart, W.M., Kellis, M., 2007b. Discovery of functional elements in 12 Drosophila genomes using evolutionary signatures. Nature 450 (7167), 219–232.

Sullivan, C.S., Ganem, D., 2005a. MicroRNAs and viral infection. Mol. Cell 20 (1), 3–7.

Sullivan, C.S., Ganem, D., 2005b. A virus-encoded inhibitor that blocks RNA interference in mammalian cells. J. Virol. 79 (12), 7371–7379.

Tabara, H., Yigit, E., Siomi, H., Mello, C.C., 2002. The dsRNA binding protein RDE-4 interacts with RDE-1, DCR-1, and a DExH-box helicase to direct RNAi in *C. elegans*. Cell 109 (7), 861–871.

Takemoto, Y., Mitsuhashi, W., Murakami, R., Konishi, H., Miyamoto, K., 2008. The N-terminal region of an entomopoxvirus fusolin is essential for the enhancement of peroral infection, whereas the C-terminal region is eliminated in digestive juice. J. Virol. 82 (24), 12406–12415.

Tang, S., Bertke, A.S., Patel, A., Wang, K., Cohen, J.I., Krause, P.R., 2008. An acutely and latently expressed herpes simplex virus 2 viral microRNA inhibits expression of ICP34.5, a viral neurovirulence factor. Proc. Natl. Acad. Sci. U. S. A. 105 (31), 10931–10936.

Terenius, O., 2008. Hemolin-A lepidopteran anti-viral defense factor? Dev. Comp. Immunol. 32 (4), 311–316.

Triboulet, R., Mari, B., Lin, Y.L., Chable-Bessia, C., Bennasser, Y., Lebrigand, K., Cardinaud, B., Maurin, T., Barbry, P., Baillat, V., Reynes, J., Corbeau, P., Jeang, K.T., Benkirane, M., 2007. Suppression of microRNA-silencing pathway by HIV-1 during virus replication. Science 315 (5818), 1579–1582.

Umbach, J.L., Kramer, M.F., Jurak, I., Karnowski, H.W., Coen, D.M., Cullen, B.R., 2008. MicroRNAs expressed by herpes simplex virus 1 during latent infection regulate viral mRNAs. Nature 454 (7205), 780–783.

Varkonyi-Gasic, E., Wu, R., Wood, M., Walton, E.F., Hellens, R.P., 2007. Protocol: a highly sensitive RT-PCR method for detection and quantification of microRNAs. Plant Methods 3, 12.

Walz, N., Christalla, T., Tessmer, U., Grundhoff, A., 2009. A global analysis of evolutionary conservation among known and predicted gammaherpesvirus microRNAs. J. Virol. 84 (2), 716–728.

Wuchty, S., Fontana, W., Hofacker, I.L., Schuster, P., 1999. Complete suboptimal folding of RNA and the stability of secondary structures. Biopolymers 49 (2), 145–165.

Yamakawa, M., Tanaka, H., 1999. Immune proteins and their gene expression in the silkworm, *Bombyx mori*. Dev. Comp. Immunol. 23 (4–5), 281–289.

Yan, X., Mouillet, J.F., Ou, Q., Sadovsky, Y., 2003. A novel domain within the DEAD-box protein DP103 is essential for transcriptional repression and helicase activity. Mol. Cell. Biol. 23 (1), 414–423.

Yi, R., Qin, Y., Macara, I.G., Cullen, B.R., 2003. Exportin-5 mediates the nuclear export of pre-microRNAs and short hairpin RNAs. Genes Dev. 17 (24), 3011–3016.

Yu, X., Zhou, Q., Li, S.C., Luo, Q., Cai, Y., Lin, W.C., Chen, H., Yang, Y., Hu, S., Yu, J., 2008. The silkworm (*Bombyx mori*) microRNAs and their expressions in multiple developmental stages. PLoS One 3 (8), e2997.

Zuker, M., Stiegler, P., 1981. Optimal computer folding of large RNA sequences using thermodynamics and auxiliary information. Nucleic Acids Res. 9 (1), 133–148.